HHS Public Access

Author manuscript

Science. Author manuscript; available in PMC 2015 September 05.

Published in final edited form as:

Science. 2014 December 5; 346(6214): 1242–1246. doi:10.1126/science.1259357.

Time-Resolved Serial Crystallography Captures High Resolution Intermediates of Photoactive Yellow Protein

Jason Tenboer[a], **Shibom Basu**[b], **Nadia Zatsepin**[c], **Kanupria Pande**[a], **Despina Milathianaki**[d], **Matthias Frank**[e], **Mark Hunter**[e], **Sébastien Boutet**[d], **Garth J. Williams**[d], **Jason E. Koglin**[d], **Dominik Oberthuer**[f], **Michael Heymann**[f], **Christopher Kupitz**[b], **Chelsie Conrad**[b], **Jesse Coe**[b], **Shatabdi Roy-Chowdhury**[b], **Uwe Weierstall**[c], **Daniel James**[c], **Dingjie Wang**[c], **Thomas Grant**[g], **Anton Barty**[f], **Oleksandr Yefanov**[f], **Jennifer Scales**[a], **Cornelius Gati**[f], **Carolin Seuring**[f], **Vukica Srajer**[h], **Robert Henning**[h], **Peter Schwander**[a], **Raimund Fromme**[b], **Abbas Ourmazd**[a], **Keith Moffat**[h,i], **Jasper Van Thor**[j], **John H. C. Spence**[c], **Petra Fromme**[b], **Henry N. Chapman**[f], and **Marius Schmidt**[a,#]

[a]University of Wisconsin-Milwaukee, Physics Department, 1900 E Kenwood Blvd, Milwaukee WI, 53211, USA

[b]Arizona State University, Department of Chemistry and Biochemistry, Tempe AZ, 85287, USA

[c]Arizona State University, Department of Physics, Tempe AZ 85287, USA

[d]Linac Coherent Light Source, SLAC National Accelerator Laboratory, Sand Hill Road, Menlo Park, CA 94025, USA

[e]Lawrence Livermore National Laboratory, Livermore, CA 94550, USA

[f]Center for Free Electron Laser Science, Deutsches Elektronen Synchrotron DESY, Notkestrasse 85, 22607 Hamburg, Germany

[g]University of New York Buffalo, Hauptman-Woodward Institute, 700 Ellicott St, Buffalo, NY 14203, USA

[h]University of Chicago, Center for Advanced Radiation Sources, 5640 S. Ellis Avenue, Chicago, IL 60637, USA

[i]University of Chicago, Department of Biochemistry & Molecular Biology and Institute for Biophysical Dynamics, 929 E. 57th Street, Chicago, IL, 60637, USA

[j]Imperial College, Faculty of Natural Sciences, Life Sciences, London SW7 2AZ, UK

Abstract

[#]Corresponding author; m-schmidt@uwm.edu.

SUPPLEMENTARY MATERIALS

www.sciencemag.org/content/

Supplementary Methods and Supplementary Text

References (35-63)

Figs. S1 – S10

Tables S1 – S4

Serial femtosecond crystallography using ultrashort pulses from X-ray Free Electron Lasers (XFELs) offers the possibility to study light-triggered dynamics of biomolecules. Using microcrystals of the blue light photoreceptor, photoactive yellow protein, as a model system, we present high resolution, time-resolved difference electron density maps of excellent quality with strong features, which allow the determination of structures of reaction intermediates to 1.6 Å resolution. These results open the way to the study of reversible and non-reversible biological reactions on time scales as short as femtoseconds under conditions which maximize the extent of reaction initiation throughout the crystal.

X-ray structure analysis has successfully determined high-resolution structures of more than 100,000 proteins and nucleic acids. But these structures represent static pictures of the biomolecules, which during their reactions engage in rapid dynamic motion. Time-resolved macromolecular crystallography (TRX) (1) unifies structure determination with protein kinetics, since both can be determined from the same set of data (2, 3). TRX is traditionally performed using pump – probe experiments and the Laue method at a synchrotron source, in which light-sensitive molecules within a crystal at near-physiological temperature are illuminated by a laser pump pulse to initiate their reaction and then by a polychromatic, probe X-ray pulse. These experiments rely on the exceptional stability of synchrotron sources to measure small, time-dependent differences between diffraction patterns with and without the pump laser pulse. Synchrotron-based Laue diffraction experiments are currently restricted by the X-ray beam brilliance to strongly scattering, relatively large (typically 6×10^5 μm^3) crystals, whose optical density makes high, uniform reaction initiation difficult. Further, the time resolution is limited to around 100 ps by the duration of the probe, X-ray pulse. However, difference electron density (DED) maps from synchrotron-based TRX experiments have revealed that large structural changes occur in times shorter than 100ps (4–7). Important structural changes associated with key chemical processes such as isomerization evidently occur in the femtosecond (fs) to tens of ps range, inaccessible to synchrotron experiments. The advent of free electron lasers such as the Linac Coherent Light Source (LCLS) and the SPring-8 Angstrom Compact free-electron LAser (SACLA) has opened a new avenue for ultrafast time-resolved structural studies. These lasers emit femtosecond pulses of hard X-rays whose peak brilliance is 10^9 times higher than that available at the most advanced synchrotrons.

The method of serial femtosecond crystallography (SFX) (8) has opened new opportunities for time-resolved structural studies (9, 10). In SFX a stream of micro- or nanocrystals in their mother liquor at near-physiological temperature is delivered by a liquid jet injector (11) to the X-ray interaction region, where the diffraction pattern of a single tiny crystal is recorded by illuminating the jet with an individual X-ray pulse from the XFEL. Diffraction patterns are obtained rapidly e.g. at 120 Hz at the LCLS. Although enormous X-ray doses, up to 1000 times greater than the room temperature synchrotron “safe dose” (12), are deposited in the crystal by the fs X-ray pulse, the processes that lead to destruction are sufficiently slow that the crystals diffract before they are destroyed (8, 13, 14). Structures are solved using thousands of diffraction patterns of individual crystals, whose diffraction patterns extend to near-atomic resolution (15, 16). To conduct a time-resolved SFX (TR-SFX) experiment at the XFEL with fs time resolution, a reaction must be initiated in a light-

sensitive crystal by a fs laser pump pulse, then probed after a time delay Δt by a fs X-ray probe pulse (9, 17).

TR-SFX is challenging due to the very different properties of the X-ray pulses emitted by synchrotrons compared to XFELs (10, 18). Time-resolved synchrotron studies take advantage of an X-ray beam with exceptional stability, where ideally a data set is collected on one large single crystal at essentially constant beam energy, bandwidth, photon flux, and volume of the crystal exposed to the X-rays. The resulting data consist of sets of consecutive light and dark images collected at the same orientation from the large single crystal. This consistency of data acquisition is important, as structure factor changes between the light and dark states are often very small. In contrast, several inherent pulse-to-pulse variations make TR-SFX at atomic resolution challenging: i) the XFEL photon flux per pulse can vary by up to an order of magnitude; ii) the peak energy and spectral content of the X-ray beam changes from pulse to pulse; iii) the crystal size is variable and even if it were constant, the volume of the crystal interacting with the beam can change. These factors give rise to large fluctuations in the diffracted intensities. However, the resulting total error is inversely proportional to the square root of the number of diffraction patterns (18) and by collecting diffraction patterns from a large number of tiny crystals, high quality X-ray data can be obtained (15, 16, 19).

Nevertheless, TR-SFX offers several advantages over time-resolved Laue crystallography at a synchrotron: i) significantly improved time-resolution, largely set by the duration of the X-ray pulse in the fs time range; ii) the diffraction-before-destroy principle overcomes the X-ray damage problem; iii) each crystal diffracts only once and crystals are rapidly exchanged, which provides an easy way to address irreversible processes; iv) the quasi-monochromatic FEL X-ray beam allows investigation of crystals with large unit cells; v) diffraction patterns are less sensitive to crystal mosaicity than in the Laue method; vi) the small size of the crystals (often <10 μm) allows more uniform laser initiation of the reaction of the molecules in the crystal. These advantages were exploited in the first TR-SFX studies of the large protein complexes, Photosystem I - ferredoxin complex and Photosystem II, as model systems (20, 21). Structural changes were recently discovered in a pump-probe TR-SFX study of the water-splitting complex in Photosystem II at 5.5Å resolution (22) but their interpretation remains provisional, in part because of the limited resolution.

We demonstrate that high-resolution, interpretable DED maps can be determined by applying TR-SFX to a well-studied model system, the bacterial blue light photoreceptor photoactive yellow protein, PYP. Upon absorption of a blue photon, PYP enters a photocycle in which numerous intermediates are occupied on timescales from femtoseconds to seconds (Fig. 1A) (23–25). Structural changes on timescales longer than 100 ps have been investigated to high resolution by time-resolved crystallography using the Laue method at synchrotrons (4, 5, 26). Even barriers of activation were determined recently solely from temperature-dependent time-resolved X-ray data (3). The photocycle examined by time-resolved crystallography contains six intermediates denoted I_T, I_{CT}, pR_1, pR_2, pB_1 and pB_2. The strongest features appear in the DED maps when pR_1 and pR_2 are substantially populated, because the sulfur of Cys69 to which the chromophore is covalently attached is significantly displaced in both these intermediates. This occurs between roughly 200 ns and

100 μs (Fig. 1B). For our TR-SFX experiments, we selected a delay time of 1μs in order to clearly reveal these features. A second dataset was collected at a time delay of 10 ns, where three distinct intermediates are significantly populated whose interpretation requires high-quality data. The DED maps are calculated from X-ray data analyzed by Monte Carlo integration over a large number of diffraction patterns, each of which is subject to all the stochastic fluctuations outlined above (18). Comparison with synchrotron Laue data establishes that the DED maps determined by the two methods are very similar. These findings open the way to high-resolution TR-SFX studies of light-driven processes and by extension, to reactions, both reversible and non-reversible, which may be initiated by other methods.

We collected TR-SFX data for the dark and excited states in an interleaved mode by using two 20 Hz ns lasers to initiate the reaction. Every third X-ray pulse probes a laser-excited crystal, resulting in a light-dark-dark scheme (Fig. S1 in the supplemental material, SM). The time-resolved data sets were obtained for pump - probe delay times of 10 ns and 1 μs, at a laser pulse energy of 15 μJ focused to a 150 μm beam diameter at the sample (~800 μJ/mm^2). The microcrystal hit rate varied between 1% and 18%, and 60% of the resulting diffraction patterns were successfully indexed (Tab. S1). Data quality as judged by the R-split values progressively improves with the number of indexed patterns (Table S2 and Fig. S4). R-split for the dark data approaches the overall value of 6.5 % for 65,000 indexed patterns, remains below 10% to ~2 Å resolution and is still acceptable (22.4%) at the highest resolution of 1.6 Å. Since the data collection scheme generated two times more dark patterns than light patterns, the light data show a somewhat larger value of R-split (9.2 % for 32,000 indexed patterns). DED maps were calculated from weighted difference structure factor amplitudes (2) with phases derived from a structural model of PYP refined against the X-ray FEL dark data (SM). The initial model was obtained from the Protein Data Bank (27) entry 2PHY. The results are shown in Figs. 2 and 3. Monte Carlo integration robustly determines intensities for the strongly-diffracting PYP crystals. Synchrotron-quality DED maps with positive and negative peaks around 10 standard deviations σ (3) are obtained with only 4000 indexed light patterns (SM). Since the unit cell of PYP crystals is relatively small and the crystals are of a few μm in size, intensity fringes between Bragg reflections caused by the shape transform of the crystals (28) are absent. In addition, the mosaicity of PYP crystals is extremely small, so that many reflections may be collected almost as full reflections. As a result, sufficiently accurate intensities are obtained from fewer diffraction patterns. Strong DED features can already be observed at very large R-split values (Tab. S2) corresponding to higher experimental noise in the structure amplitudes. If the noise in the amplitudes is too high, DED features deteriorate (29, 30). To extract faint DED features associated with small structural changes of PYP, diffraction patterns should preferably be collected with a laser-on, laser-off sequence to accumulate an equal number of light and dark patterns, aiming for redundancies on the order of 1500 in the highest resolution shell.

Fig. 2 shows an overview of the 1 μs light minus dark DED map superimposed on the refined PYP dark structure. The largest DED peak is located on the sulfur of the chromophore (Fig. 2A) and has a highly significant negative value of −22σ (where σ is the rms value of the DED across the asymmetric unit). The largest positive DED peak (18σ) is close to the same sulfur. These features reveal substantial displacement of the sulfur 1 μs

after laser excitation, associated with change in the chromophore configuration from *trans* to *cis*. Chromophore isomerization triggers further protein conformational changes extending to the periphery of the protein (red arrow). The positive (blue) and negative (red) DED peaks are contiguous and can be interpreted in terms of atomic models (Figs. 3B, and C). When the resolution is reduced below 3 Å, the difference signal disappears (Fig. S7) and clear interpretation of structural changes in PYP becomes no longer possible. We note, however, that the minimum resolution needed to observe structural changes is likely system-dependent, and an extension to other systems must await further work.

Figs. 3A and D compare the electron densities of the dark PYP structure derived from SFX with those from the Laue method. The maps are of comparable quality and can be interpreted by the same reference structure (yellow). Figs. 3B and C show the DED maps obtained at 10 ns and 1 μs time delays from TR-SFX data. The DED maps are initially interpretable with intermediate structures derived from our earlier Laue experiments at BioCARS beamline 14-ID at the Advanced Photon Source (3, 4, 26). Negative DED features in both panels are accounted for by the yellow reference (dark) structure. Each DED map arises from a mixture of intermediates. For the 10 ns map, we show here only the I_{CT} intermediate (4) in green as a guide to the eye. Figs. 3D–F show corresponding maps collected by Laue diffraction at 0 °C. The Laue 32 ns DED map correlates well with the 10 ns TR-SFX map. Many features are present in both the TR-SFX and Laue maps, and it is evident that they show the same mixture of intermediates. Particularly intriguing is the displacement of Glu46 caused by the initial isomerization of the chromophore, shown in both maps. It should be noted that the mixture of intermediates, whose concentrations change rapidly around 10 ns, prevents the refinement of individual intermediate structures until a complete time series of DED maps (3–5, 26) becomes available. In the 1 μs map (Fig. 3C), two intermediates pR_1 and pR_2 are present with significant occupancy (orange and pink structures, respectively). Since the concentration of these intermediates does not change over several decades in time (Fig. S5A), structural characterization of this mixture is possible. The refinement of this mixture with an appropriate pair of conformations reveals hitherto unidentified structural changes (compare Fig. S8A with Fig. S9). In the TR-SFX maps, the DED features are much more pronounced with stronger positive and negative features which are also much better connected spatially, and thus are more readily interpretable than the Laue maps.

The fraction of molecules that entered the photocycle can be determined by fitting calculated DED maps of the two intermediates populated at the 1 μs time delay to the observed DED map (SM). About 22% of the molecules populate the pR_2 intermediate and 18% the pR_1. The extent of reaction initiation by the ns laser pulse is therefore 40%, which is 3 to 4 times higher than the 10–15% typically achieved in synchrotron experiments (3). The higher extent of reaction initiation with the smaller crystals used in TR-SFX demonstrates one of its key advantages for time-resolved studies, and provides an explanation for the higher quality DED maps.

The conditions for pump laser and X-ray probe differ significantly between Laue and TR-SFX experiments. In a time-resolved Laue experiment on a large single crystal of PYP, 3 to 10 complete pump-probe sequences, with waiting times of a few seconds between each

sequence to allow completion of the photocycle, are necessary to accumulate a sufficiently exposed diffraction pattern prior to detector readout. When the ns laser is used for reaction initiation, the laser beam is usually smaller than the crystal size and does not penetrate fully and uniformly through the large, optically dense crystals. This localized application of the repeated, intense laser pulses induces transient strain in the crystals, which results in radially-streaked Laue spots. Strain imposes an upper limit on the useful laser energy, which for PYP crystals is around 4 to 5 mJ/mm^2 at 485 nm. This sets a practical limit on the extent of reaction initiation. Further, the repeated laser pulses have a damaging effect on the crystals, which imposes a limit on the total number of laser pulses that a crystal can tolerate (31). Importantly, neither limit applies to TR-SFX. Because the crystals are so small, the laser pulse can easily penetrate through them. For example, the absorption length at 450 nm where the crystal is most optically dense is about 3 μm (3). Most crystals used in this study are smaller and can be near-uniformly illuminated with little local strain. The quasi-monochromatic collimated X-ray beam results in a sharp intersection of the Ewald sphere with each reciprocal lattice point. Even if the crystal mosaicity were to increase transiently, it would only increase the extent of partiality of each spot. Indeed, radially-streaked diffraction spots do not appear in our data. In TR-SFX, each microcrystal is illuminated only once by the laser pulse, which allows the laser pulse energy to be increased to otherwise unacceptable levels. For example, the 0.8 mJ/mm^2 laser energy density at 450 nm employed here would produce irreversible bleaching if applied in a few, repetitive pulses to macroscopic crystals (32). Once excited, more than 80% of the PYP molecules return to their dark state on the ps time scale without entering the photocycle (24, 33). At the laser pulse power we employed, each molecule in the microcrystals is matched by an average of about 24 photons. Thus, each PYP molecule has the potential to be repeatedly activated within the ns pulse. Since the excited state lifetime is about 500 fs (24), the effective photolysis yield with our ns laser may in principle reach levels several times the primary quantum yield (Fig. S6). The intermediates earlier in the photocycle with lifetimes of up to 10 ns have red-shifted absorption maxima around 500 nm (25). Since we excite at 450 nm, the probability that one of these intermediates absorbs a second laser photon is negligible. Despite the very high ns laser flux, no sign of photo-induced damage is evident in our TR-SFX diffraction patterns. As a result, excellent DED maps are obtained of the quality needed for structural interpretation.

The way is now open to study reactions with ultrafast time resolution (24). For example, using fs laser pump pulses to initiate the reaction in PYP may allow time resolution in the sub-ps regime, as recently demonstrated by wide angle X-ray scattering experiments on a bacterial photosynthetic reaction center at LCLS (17). Reaching this time resolution would take structural biology into uncharted territory (24). PYP displays rich femtosecond chemistry, but little is known experimentally about the corresponding atomic structures and the way the elementary chemical process of isomerization proceeds. Moreover, on the fs timescale coherent phenomena may become evident that bear on how the PYP chromophore undergoes its primary photoabsorption. On the ultrafast timescale, the penetration depth under intense femtosecond optical excitation may be dominated by nonlinear cross-sections, while the photolysis yield becomes fundamentally limited by the primary quantum yield of the PYP chromophore. Intense optical pulses with very short duration (e.g. 10 fs) will create

only small population levels, which might be significantly increased by stretching and shaping the laser pulse (24). To capture this small population, every X-ray pulse must probe a crystal – such as a microcrystal - that has been excited as completely as possible. These experiments may elucidate the elementary mechanism of light absorption in chromophores, with implications for photosynthesis, light-sensing and the process of vision.

Our results establish that high resolution TR-SFX is readily possible. Reaction initiation by light to explore fast and ultrafast isomerization might be extended in the future to chemically-triggered reactions, which would open the door to the application of high-resolution TR-SFX at X-ray laser sources to a wide range of biologically and pharmaceutically important proteins.

Supplementary Material

Refer to Web version on PubMed Central for supplementary material.

Acknowledgments

This work was supported by NSF-STC “Biology with X-ray Lasers” (NSF-1231306). MS is also supported by NSF-0952643 (Career). The work of PF and her team is also supported by NIH grant R01GM095583. The work of MF and his team was performed in part under the auspices of the US Department of Energy by Lawrence Livermore National Laboratory under contract DE-AC52-07NA27344 and supported by LLNL Lab-Directed Research and Development Project 012-ERD-031. VS, RH and KM are supported by NIH grant R24GM111072. We are grateful to T. White for making the newest version of CrystFEL available to us. We thank R. G. Sierra and H. DeMirci (pulse institute, SLAC) for help to setup crystal preparation in their labs. We acknowledge help of Dan Deponte (LCLS) with the injector setup. M.S. is grateful to Raymond Hovey (UW-Milwaukee) and Shailesh Tripathi (Univ. of Maryland) for help on early attempts to produce microcrystals. The TR-SFX measurements were carried out at the Linac Coherent Light Source (LCLS) at SLAC National Accelerator Laboratory. LCLS is an Office of Science User Facility operated for the US Department of Energy Office of Science by Stanford University. Coordinates and (difference) structure factors are deposited in the protein data bank under accession numbers 4WL9 and 4WLA.

References

1. Moffat K. Time-resolved macromolecular crystallography. Annual review of biophysics and biophysical chemistry. 1989; 18:309.
2. Schmidt, M. Structure based enzyme kinetics by time-resolved X-ray crystallography, in: ultrashort laser pulses in medicine and biology. In: Zinth, W.; Braun, M.; Gilch, P., editors. Biological and medical physics, biomedical engineering. Berlin ; New York: Springer; Germany: 2008. p. c2008
3. Schmidt M, et al. Protein energy landscapes determined by five-dimensional crystallography. Acta Crystallogr D. Dec.2013 69:2534. [PubMed: 24311594]
4. Jung YO, et al. Volume-conserving trans-cis isomerization pathways in photoactive yellow protein visualized by picosecond X-ray crystallography. Nature chemistry. Mar.2013 5:212.
5. Schotte F, et al. Watching a signaling protein function in real time via 100-ps time-resolved Laue crystallography. Proceedings of the National Academy of Sciences of the United States of America. Nov 20.2012 109:19256. [PubMed: 23132943]
6. Schotte F, et al. Watching a protein as it functions with 150-ps time-resolved x-ray crystallography. Science. Jun 20.2003 300:1944. [PubMed: 12817148]
7. Bourgeois D, et al. Extended subnanosecond structural dynamics of myoglobin revealed by Laue crystallography. Proceedings of the National Academy of Sciences of the United States of America. Mar 28.2006 103:4924. [PubMed: 16547137]
8. Chapman HN, et al. Femtosecond X-ray protein nanocrystallography. Nature. Feb 3.2011 470:73. [PubMed: 21293373]

9. Spence JCH, Weierstall U, Chapman HN. X-ray lasers for structural and dynamic biology. Rep Prog Phys. Oct.2012 75
10. Neutze R, Moffat K. Time-resolved structural studies at synchrotrons and X-ray free electron lasers: opportunities and challenges. Current opinion in structural biology. Oct.2012 22:651. [PubMed: 23021004]
11. Weierstall U, Spence JC, Doak RB. Injector for scattering measurements on fully solvated biospecies. The Review of scientific instruments. Mar.2012 83:035108. [PubMed: 22462961]
12. Lomb L, et al. Radiation damage in protein serial femtosecond crystallography using an x-ray free-electron laser. Physical review B, Condensed matter and materials physics. Dec 1.2011 84:214111.
13. Barty A, et al. Self-terminating diffraction gates femtosecond X-ray nanocrystallography measurements. Nat Photonics. Jan.2012 6:35. [PubMed: 24078834]
14. Neutze R, Wouts R, van der Spoel D, Weckert E, Hajdu J. Potential for biomolecular imaging with femtosecond X-ray pulses. Nature. Aug 17.2000 406:752. [PubMed: 10963603]
15. Boutet S, et al. High-resolution protein structure determination by serial femtosecond crystallography. Science. Jul 20.2012 337:362. [PubMed: 22653729]
16. Redecke L, et al. Natively Inhibited Trypanosoma brucei cathepsin B structure determined by using an X-ray laser. Science. Nov 29.2012
17. Arnlund D, et al. Visualizing a protein quake with time-resolved X-ray scattering at a free-electron laser. Nature methods. Sep.2014 11:923. [PubMed: 25108686]
18. Kirian RA, et al. Structure-factor analysis of femtosecond microdiffraction patterns from protein nanocrystals. Acta crystallographica Section A, Foundations of crystallography. Mar.2011 67:131.
19. Barends TR, et al. De novo protein crystal structure determination from X-ray free-electron laser data. Nature. Jan 9.2014 505:244. [PubMed: 24270807]
20. Aquila A, et al. Time-resolved protein nanocrystallography using an X-ray free-electron laser. Optics express. Jan 30.2012 20:2706. [PubMed: 22330507]
21. Kern J, et al. Simultaneous femtosecond X-ray spectroscopy and diffraction of photosystem II at room temperature. Science. Apr 26.2013 340:491. [PubMed: 23413188]
22. Kupitz C, et al. Serial time-resolved crystallography of photosystem II using a femtosecond X-ray laser. Nature. 2014; 513:5. [PubMed: 25186866]
23. van Wilderen LJ, et al. Ultrafast infrared spectroscopy reveals a key step for successful entry into the photocycle for photoactive yellow protein. Proceedings of the National Academy of Sciences of the United States of America. Oct 10.2006 103:15050. [PubMed: 17015839]
24. Lincoln CN, Fitzpatrick AE, van Thor JJ. Photoisomerisation quantum yield and non-linear cross-sections with femtosecond excitation of the photoactive yellow protein. Physical chemistry chemical physics : PCCP. Dec 5.2012 14:15752. [PubMed: 23090503]
25. Ujj L, et al. New photocycle intermediates in the photoactive yellow protein from Ectothiorhodospira halophila: picosecond transient absorption spectroscopy. Biophysical journal. Jul.1998 75:406. [PubMed: 9649398]
26. Ihee H, et al. Visualizing reaction pathways in photoactive yellow protein from nanoseconds to seconds. Proceedings of the National Academy of Sciences of the United States of America. May 17.2005 102:7145. [PubMed: 15870207]
27. Berman HM, et al. The Protein Data Bank. Acta crystallographica Section D, Biological crystallography. Jun.2002 58:899.
28. Spence JC, et al. Phasing of coherent femtosecond X-ray diffraction from size-varying nanocrystals. Optics express. Feb 14.2011 19:2866. [PubMed: 21369108]
29. van Thor J, et al. Signal to noise considerations for single crystal femtosecond time resolved crystallography of the Photoactive Yellow Protein. Faraday discussions. 2014
30. Schmidt M, Rajagopal S, Ren Z, Moffat K. Application of singular value decomposition to the analysis of time-resolved macromolecular X-ray data. Biophysical journal. Mar.2003 84:2112. [PubMed: 12609912]
31. Schmidt M, Srajer V, Purwar N, Tripathi S. The kinetic dose limit in room-temperature time-resolved macromolecular crystallography. J Synchrotron Radiat. Mar.2012 19:264. [PubMed: 22338689]

32. Purwar N, Tenboer J, Tripathi S, Schmidt M. Spectroscopic studies of model photo-receptors: Validation of a nanosecond time-resolved micro-spectrophotometer design using photoactive yellow protein and alfa-phycoerythrocyanin. International Journal of Molecular Sciences. 2013; 14:17.

33. Groenhof G, et al. Photoactivation of the photoactive yellow protein: why photon absorption triggers a trans-to-cis Isomerization of the chromophore in the protein. Journal of the American Chemical Society. Apr 7.2004 126:4228. [PubMed: 15053611]

34. Kim TW, et al. Protein structural dynamics of photoactive yellow protein in solution revealed by pump-probe X-ray solution scattering. Journal of the American Chemical Society. Feb 15.2012 134:3145. [PubMed: 22304441]

Synopsis

Structural changes during a macromolecular reaction are accurately captured at near-atomic resolution by femtosecond pulses from an X-ray free electron laser.

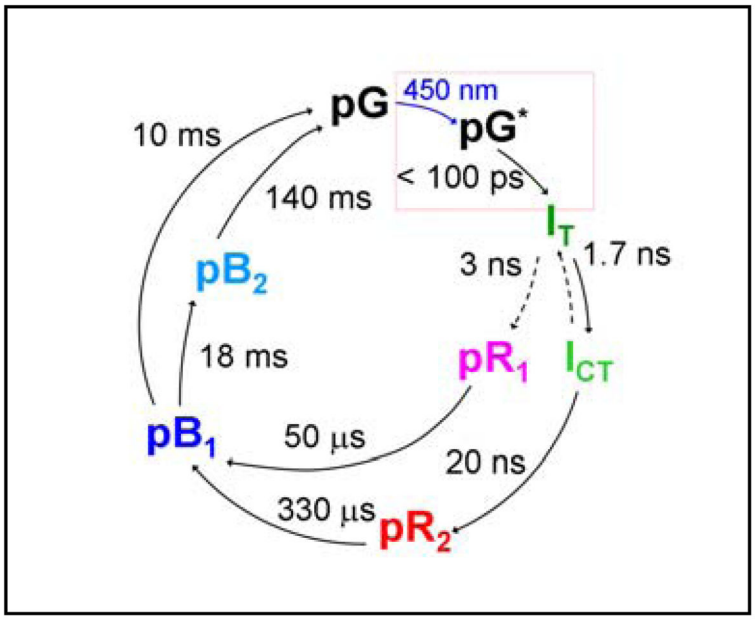

Figure 1.

Simplified PYP photocycle from the perspective of a time-resolved crystallographer (3, 4, 26). The dark state pG is activated by absorption of a blue photon (450 nm) to pG^* that begins the photocycle. The crystal structures of longer-lived intermediate states I_T, I_{CT}, pR_1 (pR_{E46Q}), pR_2 (pR_{cw}), pB_1 and pB_2 are known.

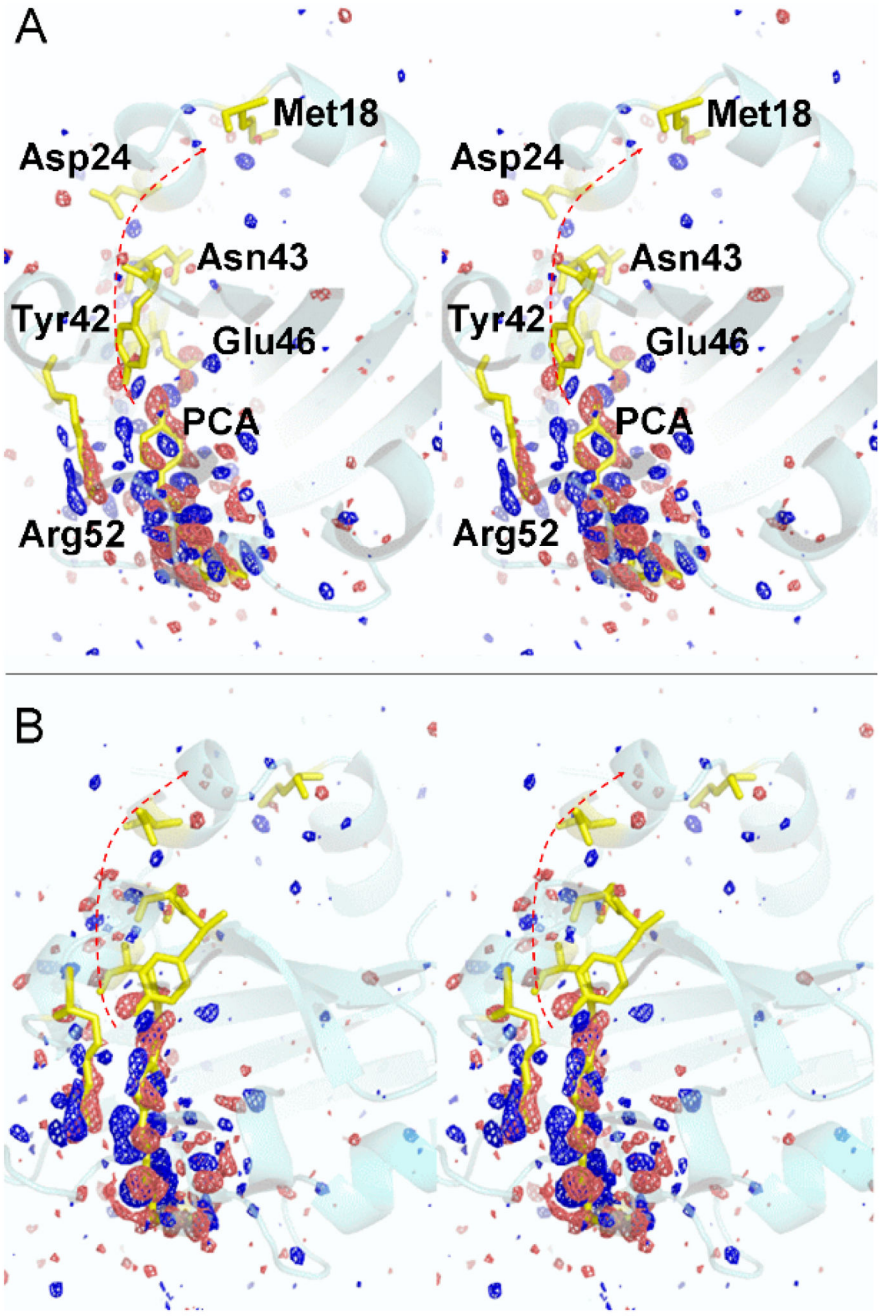

Figure 2.

Stereo view of the light - dark 1.6 Å difference electron density map at 1μs time delay, superimposed on the dark PYP structure (cyan). Contour levels: red/blue −3σ/+3σ. Chromophore and some important chromophore pocket residues are shown in yellow and marked in **A. A** Red arrow: plume of structural displacements extends to Met18, close to the N-terminal helix, which may be strongly displaced at longer times (26, 34). **B** View rotated by ~90°. A large part of the molecule does not display significant DED features and remains structurally unaltered.

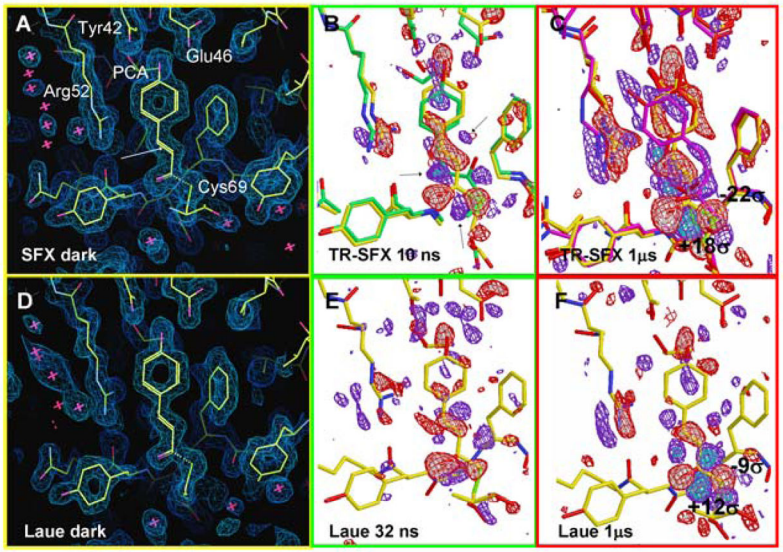

Figure 3.

Comparison of electron density and difference electron density (DED) maps in the chromophore pocket obtained by time-resolved femtosecond serial crystallography (TR-SFX) and the Laue method. The dark state is shown in yellow in all maps. **A** and **D**: Electron density maps for the PYP dark state, TR-SFX and Laue, respectively (contour level 1.1 σ, 1.6Å resolution). The PCA chromophore and nearby residues are marked in **A**. Arrow: Double bond in the chromophore about which isomerization occurs. **B** TR-SFX DED map at 10 ns. Light green structure: I_{CT} intermediate. Features marked by dotted arrows belong to additional intermediates, not shown. **C** TR-SFX DED map at 1 µs. Pink and red structures: structures of pR_1 and pR_2 intermediates, respectively. **E** Laue 32 ns DED map correlates best to the TR-SFX 10 ns map. **F** Laue 1 µs DED map. Contour levels of the DED maps: red/white −3σ/−4σ, blue/cyan +3σ/+5σ, except for **C** where cyan is +7σ. Note, **B** and **C** are displayed in stereo in the SM.